Spin-flip transitions in ^{16}O and ^{18}O excited by inelastic proton scattering

C. Djalali,* G. M. Crawley, B. A. Brown, V. Rotberg, G. Caskey,† and A. Galonsky
National Superconducting Cyclotron Laboratory and Department of Physics and Astronomy, Michigan State University, East Lansing, Michigan 48824

N. Marty, M. Morlet, and A. Willis
Institut de Physique Nucléaire, 91406 Orsay, France
(Received 8 December 1986)

Inelastic proton scattering at forward angles has been carried out on ^{16}O and ^{18}O at a bombarding energy of 201 MeV. The (p,p') spin-flip transitions to 1^+ and 2^- states are compared with (e,e'), (p,γ), and charge exchange data, and with microscopic distorted-wave Born approximation calculations using shell model wave functions. The ratios of orbital to spin contributions are deduced for the known 1^+ states in ^{16}O.

I. INTRODUCTION

During the last few years, an impressive breakthrough in our understanding of spin-isospin modes of excitation in nuclei has been achieved both experimentally and theoretically. $M1$ transitions have been extensively studied in a large number of nuclei by different selective probes such as (e,e'),[1] (γ,γ'),[2] and (p,p') (Ref. 3) reactions. A common property of such excitations is that the observed strength is generally quenched (up to a factor of 3 in some nuclei), as compared to standard shell model predictions. Different mechanisms have been proposed to explain this quenching, including the admixture with high-lying many particle—many hole configurations via the tensor force[4] or virtual (Δ-h) excitations.[5] It should be noted, however, that the amount of missing $M1$ strength that can be attributed to these high order mechanisms depends strongly on how accurately the lowest order effects, such as configuration mixing within the lowest major shells or ground state correlations, are included in the model calculations. The importance of such effects is clearly seen in doubly closed shell nuclei such as ^{16}O and ^{40}Ca. In the independent particle model, the ground states of these nuclei consist of filled shells of both spin-orbit partners and therefore $0\hbar\omega$ single particle 1^+ states cannot occur; they become possible, however, through two particle—two hole components in the ground state wave function. The study of $M1$ transitions in closed shell nuclei provides a clear test and direct measure of $2\hbar\omega$, $4\hbar\omega$, etc. correlations in the ground state wave function.

Extensive studies of the $M1$ strength distribution in the oxygen, isotopes have been carried out by (e,e') (Refs. 6 and 7) and (p,γ) (Ref. 8) reactions; this motivated us to carry out the (p,p') measurements for comparison. The excitation of 1^+ states by the electromagnetic interaction involves both a spin and an orbital contribution, whereas the hadronic interaction at small momentum transfer only has a spin part. Such comparisons in relative intensities have been made for the calcium isotopes,[9] where there is agreement for some transitions, but noticeable disagreement in other cases. In a simple model, the oxygen isotopes, like the calcium isotopes, are built by adding neutrons to a doubly closed shell, and one might therefore except similar effects in these nuclei. For some particular 1^+ states,[10] the comparison between the excitation of the same transition by (p,p') and (e,e') reactions allows a determination of the orbital and spin contributions to the electromagnetic transition probability.

An additional motivation for the present work was provided by the fact that shell model calculations (for 1^+ and 2^- states), which have been reasonably successful in describing nuclei in the beginning of the s-d shell, were available for the oxygen isotopes. By comparison with our results and previous (e,e') results, these models can be tested and the ratio of experiment to theory for the total 1^+ and 2^- strength can be obtained.

In this paper, we report on 201 MeV (p,p') scattering at forward angles on ^{16}O and ^{18}O with particular emphasis on 1^+ and 2^- states. The use of gaseous targets and the data reduction are described in Secs. II and III. A description of the shell model wave functions used is given in Sec. IV. Finally, in Sec. V the results obtained in the present work are discussed and compared to other experimental data.

II. EXPERIMENTAL PROCEDURE

The measurements were carried out using a 201 MeV proton beam from the Orsay synchrocyclotron. The general experimental arrangement to obtain proton spectra at angles as small as 2° with very low background has been described previously.[11] The unique new feature of the present measurements was the use of a gas target. Natural oxygen gas was used for the ^{16}O target (99.79% ^{16}O), and an enriched gas was used for the ^{18}O target, consisting of 98.0% ^{18}O, 1.4% ^{16}O, 0.6% ^{17}O, and other contaminants. The gas was contained in a short metallic cylinder having its symmetry axis along the beam direction and with entrance and exit windows made of thin Kapton $(C_{22}H_{10}N_2O_4)_n$ foils. In contrast to the case of solid targets which are, in general, 10—20 μm thick, the relatively large length of the gas cell along the beam axis (of the or-

der of a few centimeters) strongly affects the energy resolution. In order to limit this geometrical effect, we used a short gas cell with sufficient gas pressure to maintain reasonable target thickness. Studies of the rupture pressure versus the window thickness were made and the optimum design consisted of windows made of double foils of 12.5 μm thick Kapton. The gas cells were operated at pressures of about 3—4 atm. At these pressures the Kapton windows bowed, giving a total effective length of the gas target of about 1.8 cm. The pressure in the gas cell was constantly monitored and regularly readjusted. Runs were taken at each angle under the same beam conditions on two identical cells, one filled with oxygen and the other filled with hydrogen at the same pressure, so that an accurate measurement of the contribution from the Kapton windows could be obtained. The target thickness was checked regularly by measuring the (p,p) scattering on the hydrogen target. The deduced target thickness for the oxygen gas ranged between 7.5 and 10.0 mg/cm^2.

Measurements were made for ^{16}O from 2° to 6° in 1° steps and at 8° and 10°, and for ^{18}O from 2° to 10° in 1° steps and at 12°. The excitation energy regions covered in the present experiment ranged from 6 to 29 MeV in ^{16}O and from 5 to 20 MeV in ^{18}O. The best energy resolution obtained at forward angles was about 75 keV (full width at half maximum). Due to geometrical effects, the energy resolution became worse as the scattering angle increased, reaching 150 keV at 12°.

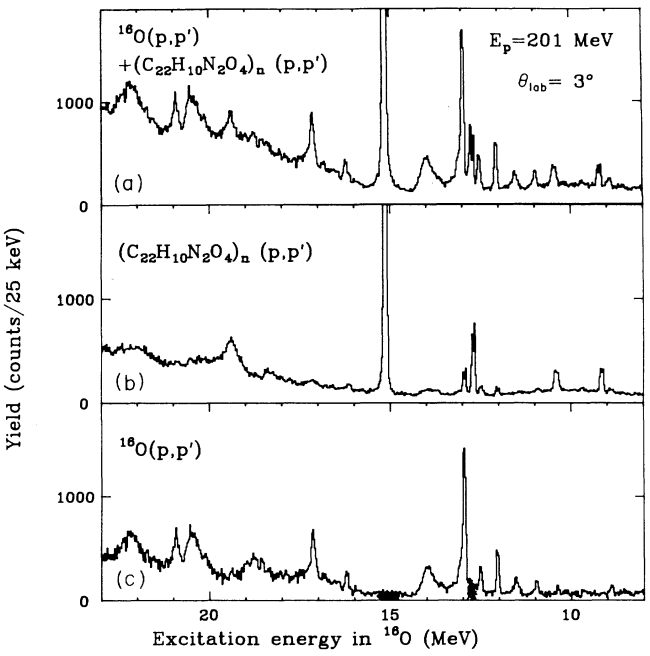

FIG. 1. (p,p') spectra measured at 3°: (a) gas cell filled with ^{16}O, (b) windows' contribution measured on a hydrogen filled gas cell, and (c) subtracted spectrum; the two regions perturbed by the subtraction are cross hatched (see text).

III. DATA ANALYSIS

Spectra measured at 3°, under the same experimental conditions, on two identical gas cells filled with ^{16}O and H, respectively, are shown in Figs. 1(a) and 1(b). The spectrum from the H filled target is mainly due to inelastic scattering on the C, and to a lesser extent on the O and N contained in the Kapton foils. The elastic (p,p) scattering on the H, contained either in the foils or in the gas cell, appears in the excitation energy region studied here only at angles greater than 8°. In the off-line analysis, at each angle, the spectrum measured on the H filled target is first normalized to the oxygen filled target spectrum using the area of the strongly excited carbon peak at 15.11 MeV, then corrected for possible shifts in energy between runs and finally subtracted channel by channel from the corresponding oxygen spectrum. The energy shifts between experimental runs are always less than 50 keV. An example of subtracted spectra for ^{16}O is given in Fig. 1(c), where the cross hatching corresponds to those portions of the spectrum which are perturbed by the subtraction of strong peaks from the carbon.

The calibration in excitation energy is deduced from known levels in ^{16}O (or ^{18}O) and by using levels of ^{12}C contained in the window foils, taking into account the kinematic shift. The calibration is good to about ±20 keV.

Absolute normalization of the cross sections is obtained by comparison with the known p-p scattering cross section at 15°, using a polyethylene target. The efficiency of the detection system is 93±2%.

The peaks or structures in the subtracted spectra are analyzed with a standard peak-stripping program. Concerning the peak shape used in the fitting procedure, two different approaches are followed. One consists of choosing, at each angle, the strongest excited state in the spectrum as the reference peak; the other approach assumes a Gaussian shape with asymmetric exponentially falling tails. Both analyses give similar results within a few percent. Broad structures are assumed, for purposes of analysis, to consist of a number of narrow peaks; if the variation with angle of the excitation energies of these peaks is comparable to the separation in energy between them, then only the summed cross sections and the centroid energy of the whole structure will be given. In the figures and the tables, the centroid energies of broad structures are given in angular brackets (⟨ ⟩).

Above the neutron emission threshold (15.66 MeV in ^{16}O and 8.04 MeV in ^{18}O, broad structures and narrow peaks appear on top of a continuum which is mainly due to many-body reactions and the tails of giant resonances. The height and shape of this continuum are generally determined empirically. At high excitation energies and for small structures, the uncertainties due to this somewhat arbitrary choice of the continuum can be as large as 30%.

IV. THEORETICAL MODELS

A. Shell model wave functions

The model spaces and interactions used for the present calculations have been discussed previously[8] and will only

be briefly summarized here. Most of the low-lying negative parity states can be understood as predominantly one-particle—one-hole excitations outside of the closed $(1s)^4(1p)^{12}$ configuration for ^{16}O. The 1p-1h configurations within this model space have been diagonalized with the residual interaction of Millener and Kurath.[12] For the low-lying positive parity excitations two-particle—two-hole and four-particle—four-hole excitations are most important. The only model space for which it is presently feasible to accommodate these excitations consists of allowing for all configurations within the three orbits $1p_{1/2}$, $1d_{5/2}$, and $2s_{1/2}$ with a closed $(1s_{1/2})^4(1p_{3/2})^8$ configuration for ^{12}C. The wave functions were obtained from the residual interactions "F" (Ref. 13) and "Z" (Ref. 14), which were determined by least squares fits to energy levels in the $A=13-18$ mass region.

For the $M1$ excitations it would clearly be desirable to include both spin-orbit partners in the valence model space, i.e., $1p_{3/2}$ and $1d_{3/2}$ in addition to $1p_{1/2}$ and $1d_{5/2}$. However, at present it seems difficult to obtain reliable excitation energies within a model space which includes the complete two-particle—two-hole basis.[8,15] This may be resolved by including four-particle—four-hole configurations, but the dimensionalities involved (of the order of 10000 for the 1^+ $T=1$ states) become too large for a straightforward calculation.

The 1^+ states in ^{18}O were calculated in the $(1p_{1/2}$-$1d_{5/2}$-$2s_{1/2})$ model space with the "F" and "Z" interactions. The results for the $M1$ strength obtained with the "Z" interaction have been reported previously.[16] In addition, the 1^+ state corresponding to the neutron transition to the $1d_{3/2}$ orbit was included by using $(sd)^2$ wave functions obtained from the new empirical interaction of Wildenthal.[17]

The percentages of zero-, two-, and four-$(p_{1/2})$ hole configurations in the ground states of ^{16}O and ^{18}O, calculated with the "F" and "Z" interactions, are given in Table I.

TABLE I. Percentage of zero, two, and four $p_{1/2}$-hole in the ground state configurations of ^{16}O and ^{18}O, calculated with the F and Z interactions described in Sec. IV.

	^{16}O		^{18}O	
$p_{1/2}$ holes	F	Z	F	Z
0	69.5	65.6	44.3	47.8
2	26.8	28.9	42.4	42.0
4	3.7	5.5	13.3	10.2

B. DWBA calculations

Microscopic DWBA (distorted-wave Born approximation) calculations for (p,p′) cross sections have been performed using the code DW81,[18] which is a modified and extended version of the code DWBA70.[19] The one body transition densities were obtained from the wave functions described above. The interaction derived by Franey and Love[20] from 210 MeV free nucleon-nucleon scattering amplitudes was used as the effective nucleon-nucleon interaction in the calculation. The optical potential used was taken from the elastic scattering data on ^{27}Al at 156 MeV.[21] It has been verified[9] for medium-heavy nuclei such as ^{40}Ca and ^{90}Zr, where the distortion effects are much more important than in the oxygen isotopes, that the (p,p′) cross sections calculated with the optical potential parameters obtained at 156 or 200 MeV are identical at forward angles ($\theta \leq 20°$) to within a few percent. The optical potential obtained by extrapolating the parametrization of Schwandt *et al.*[22] to $A=16$ and $E=200$ MeV also gives very similar results.

C. Comparison between (p,p′) and (e,e′) results

Assuming the impulse approximation and following the notation of Refs. 9 and 23, the (p,p′) cross section for exciting a 1^+ state at small momentum transfer ($q \approx 0$) can be factorized as follows:

$$\frac{d\sigma}{d\Omega}(q\approx 0) = (\mu/2\pi\hbar^2)^2 (k_f/k_i) N_D \mid V_{\text{int}} \mid^2 \times \left| \left\langle f \left| \left| \sum_k \sigma_k \tau_k \right| \right| i \right\rangle \right|^2 , \quad (1)$$

where N_D is a distortion factor and $\mid V_{\text{int}} \mid$ is the modulus of the nucleon-nucleon interaction responsible for the transition ($V_{\sigma\tau}$ for 1^+, $\Delta T=1$; V_σ for 1^+, $\Delta T=0$; etc.).

From electron scattering data, one deduces the transition probability:

$$B(M1)\uparrow = \left| (3/16\pi)^{1/2} (g_s/2) \left\langle f \left| \left| \sum_k \sigma_k \tau_k \right| \right| i \right\rangle + (3/16\pi)^{1/2} g_l \left\langle f \left| \left| \sum_k l_k \tau_k \right| \right| i \right\rangle \right|^2 = \mid \sqrt{B(\sigma)} + \sqrt{B(l)} \mid^2 , \quad (2)$$

where g_s and g_l are the spin and orbital gyromagnetic factors.

Using the shape of the calculated angular distribution, one can extrapolate the measured (p,p′) cross sections to $q \approx 0$ and deduce the value of the square of the reduced matrix element which appears on the right hand side of Eq. (1). This matrix element is directly related to the spin component $B(\sigma)$ of the transition probability $B(M1)$. Therefore, by combining (p,p′) and (e,e′) measurements, one can deduce from Eqs. (1) and (2) two values for the ratio of orbital to spin amplitudes, $\sqrt{B(l)}/\sqrt{B(\sigma)}$, depending on the relative phase between $\sqrt{B(l)}$ and $\sqrt{B(\sigma)}$.

D. Comparison between (p,p′) and (p,n) results

If the impulse approximation is assumed, the (p,n) cross section for exciting a Gamow-Teller (GT) transition at 0° ($q \approx 0$) can be factorized in a way similar to that given in Eq. (1),[23] the nucleon-nucleon interaction being $V_{\sigma\tau}$. Therefore, the (p,n) cross section at 0° for exciting a GT transition (1^+, $T=T_0$) can be simply related to the (p,p′)

cross section for exciting the analog (1^+, $T=T_0$) state in the parent nucleus, at the same momentum transfer q,

$$\frac{d\sigma}{d\Omega}(q)_{(\mathrm{p,p'})} = (T_0/2)(N_D^{\mathrm{p,p'}}/N_D^{\mathrm{p,n}}) \times |V_{\mathrm{int}}^{\mathrm{p,p'}}/V_{\sigma\tau}|^2 \frac{d\sigma}{d\Omega}(q)_{(\mathrm{p,n})} . \quad (3)$$

The distortion factor for (p,p') scattering on the oxygen isotopes is obtained as the ratio of distorted wave to plane wave cross sections at 0° calculated for the strongest 1^+ states predicted by the shell model calculations. Using the optical potentials described previously, we obtain $N_D^{\mathrm{p,p'}}=0.50\pm0.05$. The modulus of the nucleon-nucleon interaction involved in the transition at small momentum transfer is calculated from the Franey-Love parametrization.[20]

V. EXPERIMENTAL RESULTS AND DISCUSSIONS

A. ^{16}O

Subtracted spectra obtained at 3° and covering the excitation energy regions from 6.5 to 15.0 and 15.0 to 28.5 MeV are shown in Figs. 2(a) and 2(b), respectively. Below 15 MeV, except for a broad structure centered at 14 MeV, all the peaks observed correspond to known transitions.[24] At higher excitation energies, beside two sharp and well isolated levels at 16.22 and 17.14 MeV, many broad structures are observed with widths ranging from 250 keV to several MeV. Of these broad structures, only the one centered at 18.7 MeV could be uniquely analyzed in terms of single levels at all angles. All these structures appear on top of a continuum, the height and shape of which were determined empirically in two different ways.

(i) Starting at the neutron threshold, the continuum was assumed to rise smoothly and join the high excitation energy region by connecting the lowest points of the spectrum [dotted curve in Fig. 2(b)].

(ii) Assuming that the broad structures observed at 22.3 and 24 MeV correspond to the main components of the giant dipole resonance (GDR), which is clearly excited in (γ,n) experiments,[25] the (p,p') spectrum above 21.5 MeV can be fairly well reproduced in shape by the (γ,n) spectrum [solid line, Fig. 2(b)] on top of a flat continuum [dashed line in Fig. 2(b)]. The continuum is assumed to fall off smoothly to the neutron threshold, with the (γ,n) spectrum superimposed on top of it. We see from the second approach that the excitation of the GDR can account completely for the (p,p') spectrum above 21.5 MeV of excitation energy. The uncertainties in cross sections due to the different choices of the underlying continuum are included in the error bars.

Angular distributions obtained for different transitions are given in Fig. 3 and compared in shape with theoretical predictions. The shape of the angular distribution at forward angles is characteristic of the transition. The only angular distributions that are forward peaked correspond to transitions to 1^+, $T=1$ and 0^+, $T=0$ states. However, there is a difference in the shape of the angular distributions, namely the typical 0^+ angular distribution decreases more rapidly and has a minimum at 7°. This is illustrated in Fig. 3 for the known 0^+ state at 12.05 MeV. In this figure the solid and dashed curves correspond, respectively, to the predicted shape for a 0^+ and a 1^+ state. In heavy nuclei where Coulomb excitation is strong, the Coulomb excited 1^+ states have a foward peaked angular distribution similar to that of a 1^+ state.[26] This is not the case in light nuclei such as oxygen, where the Coulomb excitation is much weaker. In ^{16}O the angular distribution of a 1^-, $T=1$ state is similar to that of a 2^-, $T=1$ state (shown in Fig. 3) and is characteristic of a $\Delta L=1$ transfer. Natural parity states of higher multipolarity, like the 2^+ state at 11.52 MeV, have angular distributions which rapidly increase with angle.

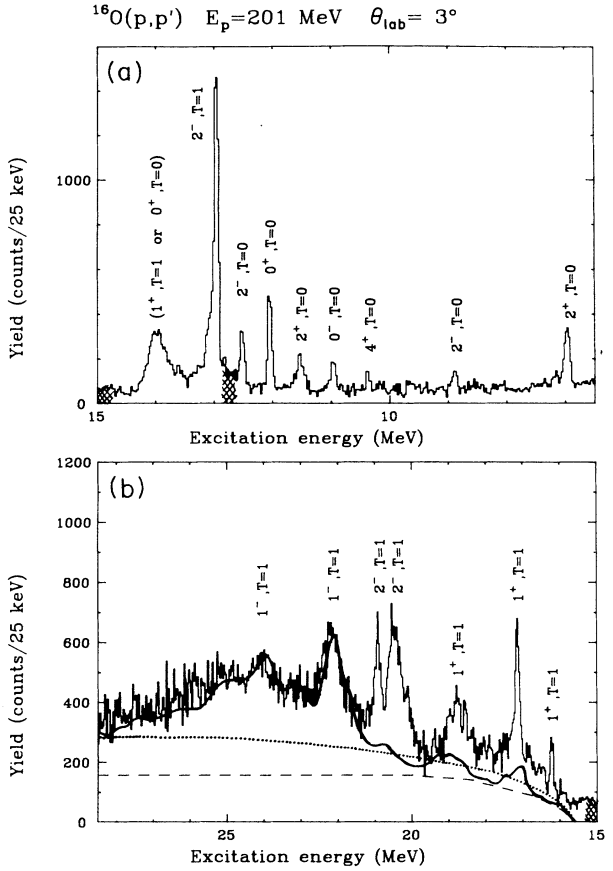

FIG. 2. ^{16}O(p,p') subtracted spectra at 3°: (a) from 6.5 to 15 MeV of excitation energy; (b) from 15.0 to 28.5 MeV of excitation energy. The dotted curve corresponds to the empirically estimated continuum. The ^{16}O(γ,n) spectrum (Ref. 25) (thick line) is shown for comparison on top of a smooth continuum (dashed line).

1. 1^+ states

The excitation energies of states having angular distributions characteristic of a 1^+, $T=1$ transition are given in Table II together with the results obtained in (e,e'),[6]

(p,γ),[8] and (p,n) (Ref. 27) reactions. The three well established 1^+ states, first observed in (p,γ) and (e,e') reactions, are clearly excited in (p,p') at 16.22, 17.14, and 18.77 MeV [Fig. 2(b)]. In the (e,e') experiment, eight additional weakly excited 1^+ states are reported between 17.4 and 18 MeV; no such states are observed in the present experiment.

Another difference with the results of previous experiments is the clear observation in the present experiment of a broad structure at 14 MeV, with a full width at half maximum of 0.4 MeV [Fig. 2(a)]. The (p,p') cross section for exciting this structure is as large as the sum of the cross sections observed for the three well known 1^+ states. It is therefore puzzling that no such 1^+ state (or analog 1^+ state) is observed in the (p,γ) [or (p,n)] reaction.

In an early (e,e') experiment,[28] a structure with a width of 170±50 keV was observed at 14 MeV and was interpreted as a 0^+ state. A 0^+ state with a width of 200±50 keV is also listed[24] at 14.03 MeV, as observed in $^{12}C + \alpha$ scattering. There is also some indication of a 0^+ state at 13.95 MeV obtained in $^{16}O(\alpha,\alpha')$ scattering.[29] However, the width measured in all these experiments is almost a factor of 2 smaller than the 400±30 keV observed in the present (p,p') experiment. Furthermore, our measured (p,p') angular distribution for the 14 MeV structure (Fig. 3) does not exhibit a minimum near 7°, as would be expected for a typical 0^+ state, such as the known 0^+ state at 12.05 MeV (Fig. 3).

It is unlikely that the 14 MeV structure is a 1^+, $T=0$ state, since the angular distributions of known 1^+, $T=0$ states are much flatter than the angular distribution for this structure. Based on the shape of the measured (p,p') angular distribution, we would conclude that the 14 MeV structure is a 1^+, $T=1$ state. However, if it were a 1^+, $T=1$ state, it should have been observed in the (p,n) or

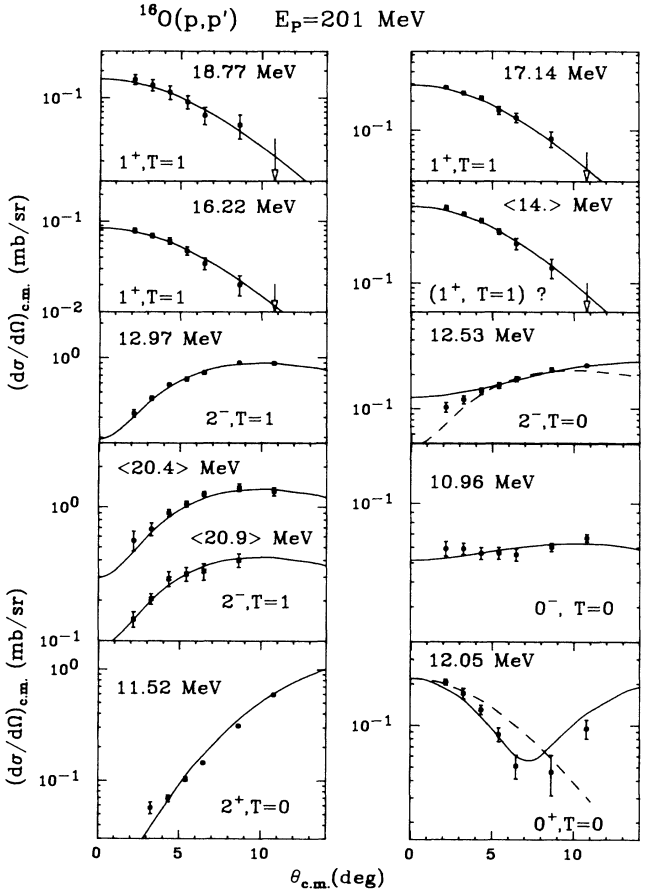

FIG. 3. Measured (p,p') angular distributions for some states in ^{16}O compared with microscopic DWBA calculations (see text for normalization factors).

TABLE II. 1^+ states observed in ^{16}O and ^{18}O by different inelastic scattering experiments. † denotes the centroid of a broad structure. †† denotes candidates for 1^+, $T=1$ states. * denotes the centroid of eight weakly excited states between 17.4 and 18 MeV. [*A*]=12.4–13.2 MeV, [*B*]=13.2–14.0 MeV, and [*C*]=14.0–15.0 MeV.

	(p,p')[a]		(e,e')[b]		(p,γ)[c]		(p,n)[d]	
	E_x (MeV)	$J^\pi;T$	E_x (MeV)	$J^\pi;T$	E_x (MeV)	$J^\pi;T$	E_x (in ^{16}F) (MeV)	$J^\pi;T$
^{16}O	⟨14.0⟩†	$(1^+;1)^{††}$						
	16.22±0.01	$1^+;1$	16.22±0.01	$1^+;1$	16.22±0.01	$1^+;1$	3.76	$1^+;1$
	17.14±0.01	$1^+;1$	17.14±0.01	$1^+;1$	17.14±0.01	$1^+;1$	4.65	$1^+;1$
			(17.7)*	$1^+;1$				
	18.77±0.01	$1^+;1$	18.79±0.01	$1^+;1$	18.8 ±0.1	$1^+;1$	6.23	$1^+;1$
^{18}O	8.82±0.01	$(1^+;1)^{††}$					9.9	$(1^+;1)^{††}$
							10.9	$(1^+;1)^{††}$
	⟨10.10⟩†	$(1^+;1)^{††}$					11.9	$(1^+;1)^{††}$
	[*A*]	$(1^+;1)^{††}$						
	[*B*]	$(1^+;1)^{††}$						
	[*C*]	$(1^+;1)^{††}$						
			18.871±0.005	$1^+,2$				

[a]Present work.
[b]Reference 6 for ^{16}O and Ref. 7 for ^{18}O,
[c]Reference 8.
[d]Reference 27 for ^{16}O and Ref. 36 for ^{18}O.

TABLE III. Comparison of (p,p′) cross sections for 1^+ states with predictions using (p,n) cross sections measured at 135 MeV. † denotes normalization by 1.76 as suggested by the authors of Ref. 38. * denotes fine structures within the 10.1 MeV broad structure.

	(p,n)[a]		(p,p′) predicted from (p,n)		(p,p′)[b]
	E_x (in ^{16}F) (MeV)	$(d\sigma/d\Omega)_{(p,n)}(0°)$ (mb/sr)	$(d\sigma/d\Omega)^{\text{predicted}}_{(p,p')}(3°)$ (mb/sr)	E_x (MeV)	$(d\sigma/d\Omega)_{(p,p')}(3°)$ (mb/sr)
^{16}O	3.76	≈0.03	≈0.2	16.22	0.07±0.01
	4.65	0.38	0.20±0.04	17.14	0.24±0.02
	6.23	0.33	0.17±0.03	18.77	0.14±0.01
	E_x (in ^{18}F) (MeV)	$(d\sigma/d\Omega)_{(p,n)}(0°)^{\dagger}$ (mb/sr)	$(d\sigma/d\Omega)^{\text{predicted}}_{(p,p')}(1.5°)$ (mb/sr)	E_x (MeV)	$(d\sigma/d\Omega)_{(p,p')}(1.5°)$ (mb/sr)
^{18}O	9.9	0.44±0.09	0.24±0.07	8.82	0.32±0.05
	10.9	0.65±0.13	0.33±0.10	9.76	0.15±0.03*
				9.89	0.16±0.03*
	11.9	0.48±0.10	0.25±0.07	10.80	0.06±0.02*

[a]On ^{16}O, Ref. 27; on ^{18}O, Ref. 36.
[b]This work.

electromagnetic measurements; on the other hand, if it were the 0^+ state suggested by some earlier measurements, first the width observed in the present experiment is too large and, second, the measured angular distribution should have a minimum near 7°. Therefore, there remains some ambiguity about the nature of this transition. Possibly a 0^+ state with a rather special radial dependence of its form factor might have an angular distribution at forward angles which is similar to that for a 1^+, $T=1$ state in ^{16}O. Spin-flip transition probability measurements on ^{16}O would help to clarify the nature of this transition.

The (p,p′) and (p,n) (Ref. 31) 1^+ cross sections measured, respectively, in ^{16}O and ^{16}F are compared in Table III. Using Eq. (3), from the measured zero degree Gamow-Teller cross section in ^{16}F, the (p,p′) cross section for the parent 1^+ state in ^{16}O has been predicted at the same momentum transfer [which, in the case of ^{16}O, corresponds to a (p,p′) scattering angle of 3°]. Except for the 16.22 MeV state, the analog of which is only weakly excited in the (p,n) reaction, the agreement between the predicted and the measured (p,p′) cross sections is very good. Relation (3) can be used the other way by predicting (p,n) cross sections from the (p,p′) results; this has been done for the 14 MeV structure, assuming that it is an $M1$ transition. The analog of this state is predicted to be excited in the 135 MeV (p,n) reaction at an excitation energy of 1.51 MeV in ^{16}F with a zero degree cross section of about 0.8 mb/sr. The fact that, as mentioned above, no such state has been observed[27] adds to the puzzle about the nature of this structure.

The 1^+, $T=1$ strength distributions measured in the present experiment and in the (e,e′) experiment are compared with theoretical predictions in Fig. 4. The comparison is limited to the excitation energy region below 20 MeV, first because in (e,e′) only the region between 16 and 20 MeV has been studied in detail, and second because above 20 MeV the 1^+ strength is expected to be very fragmented and especially difficult to detect in (p,p′), where the GDR is so strongly excited. In Fig. 4, the (p,p′) strength measured at 14 MeV has been assumed to be distributed over several single states simply to reproduce the shape of the structure. Both calculations predict almost the same total 1^+ strength up to 20 MeV of excitation energy; however, the strength distribution depends strongly on the interaction used. With the Z interaction, more than 80% of the total strength is concentrated in two

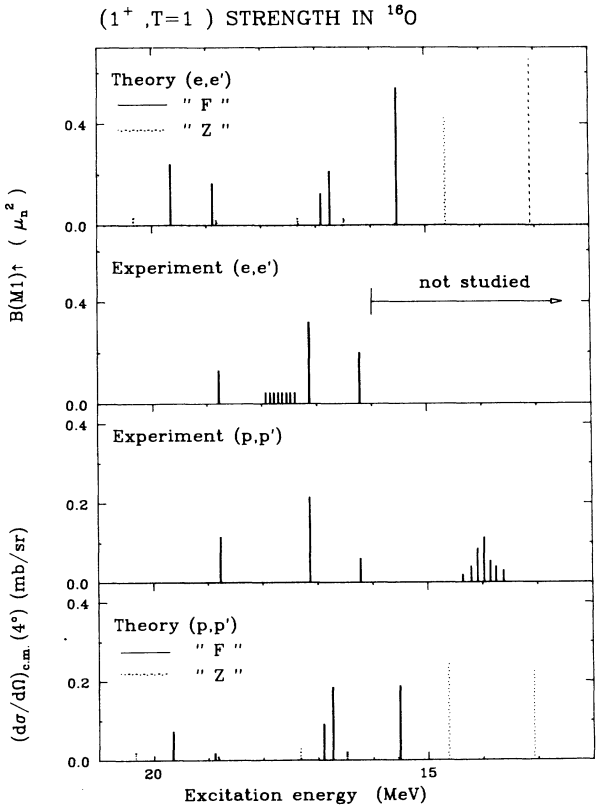

FIG. 4. (p,p′) and (e,e′) predicted strength distributions for 1^+, $T=1$ states in ^{16}O (see Sec. IV) compared with the measured ones [this work and Ref. 6 for (e,e′)].

TABLE IV. Spin transition probabilities $B(\sigma)$ and orbital to spin ratios $|\sqrt{B(l)}/\sqrt{B(\sigma)}|$ for 1^+ states in ^{16}O and ^{18}O, deduced from the comparison between (e,e′) and (p,p′) results. † denotes the centroid of a broad structure. * (**) denotes constructive (destructive) interference between $\sqrt{B(l)}$ and $\sqrt{B(\sigma)}$.

	E_x (MeV)	$(d\sigma/d\Omega)_{p,p'}(q\approx 0)$[a] (mb/sr)	$B(\sigma)\uparrow$[a] (μ_N^2)	$B(M1)\uparrow$ (μ_N^2) (e,e′)[b]	(μ_N^2) (p,γ)[c]	$\lvert\sqrt{B(l)}/\sqrt{B(\sigma)}\rvert$ (range)
^{16}O	⟨14.0⟩†	$(6.28\pm0.45)\times10^{-1}$	0.54±0.04			
	16.22	$(9.52\pm0.93)\times10^{-2}$	0.08±0.01	0.20±0.02	0.22±0.02	0.41—0.77*
						2.41—2.77**
	17.14	$(3.49\pm0.24)\times10^{-1}$	0.30±0.03	0.32±0.03	0.33±0.04	0.03—0.14*
						1.94—2.14**
	18.77	$(1.96\pm0.18)\times10^{-1}$	0.17±0.02	0.13±0.03	0.14±0.02	0.03—0.27*
						1.72—2.03**
^{18}O	8.82	$(3.50\pm0.20)\times10^{-1}$	0.18±0.03			
	⟨10.10⟩†	1.62±0.05	0.83±0.11			
	18.87	$<6\times10^{-2}$	<0.05	0.28±0.04		≧1.20—1.50*
						≧3.20—3.50**

[a]This work.
[b]Reference 6 for ^{16}O and Ref. 7 for ^{18}O.
[c]Only for ^{16}O, Ref. 8.

strong states at 13.08 and 14.64 MeV. In the calculation with the F interaction, the strength is distributed over five states between 15 and 20 MeV. The centroid energy of the predicted strength below 20 MeV is almost the same for (p,p′) and (e,e′); it is equal to 14.3 MeV using the Z interaction and 17 MeV using the F interaction. These values are to be compared with the experimental ones, which are 17.4 MeV for (e,e′) and 17.5 and 15.8 MeV for (p,p′), depending on whether the 14 MeV strength is included in the total strength or not. Experimentally, there are fewer differences in relative intensities between (p,p′) and (e,e′) for the well known 1^+ states than are expected from the models. For most of the 1^+ states, both calculations predict a significant orbital contribution which interferes constructively with the spin term in the (e,e′) reaction.

The predicted ratio of orbital to spin amplitudes $[\sqrt{B(l)}/\sqrt{B(\sigma)}]$ varies from state to state and is in the range 0.1—1.7 using the F interaction and 0.6—1.3 using the Z interaction. Following the procedure described in Sec. IV C, we have deduced for the well established 1^+ states two different ranges of values for the ratio of orbital to spin amplitudes, depending on the relative phase between these amplitudes. These ratios are given in Table IV. If we assume, as suggested by the models, constructive interference between the orbital and the spin ampli-

TABLE V. Ratio of the measured 1^+ strength to the total predicted strength (summed up to 20 MeV of excitation energy) for individual transitions and their sum, in ^{16}O. † denotes the centroid of eight weakly excited states between 17.4 and 18 MeV. * denotes a nature not well established.

	Measured strength divided by total predicted strength for $M1$ states			
	F		Z	
E_x	(p,p′)[a]	(e,e′)[b]	(p,p′)[a]	(e,e′)[b]
⟨14.0⟩[a,*]	0.73		0.65	
16.22[a,b]	0.12	0.15	0.10	0.14
17.14[a,b]	0.38	0.23	0.34	0.21
⟨17.7⟩[†,b,*]		0.27		0.25
18.77[a,b]	0.21	0.10	0.19	0.09
$\sum$, three well established 1^+ states observed in both a and b	0.71±0.06	0.48±0.06	0.63±0.05	0.44±0.05
$\sum$, all 1^+ states listed above	1.44±0.11	0.75±0.13	1.28±0.10	0.69±0.12

[a]This work.
[b](e,e′), Ref. 6.

tudes, we see that only the state at 16.22 MeV has an orbital contribution that is significant; it is 2—3 times larger than for the two other states. Assuming that the 14 MeV structure is a 1^+ state, we obtain a large spin transition probability $B(\sigma)=0.54\ \mu_N^2$. Therefore, its nonobservation in (p,γ) reaction would imply a very large orbital contribution which, contrary to the theoretical predictions, would have to interfere destructively with the spin term.

The measured 1^+ strengths for (p,p') and (e,e') are compared to the total predicted strength below 20 MeV in Table V, where the ratio of experiment to theory is given for the individual states as well as for their sum. If we consider only the states at 16.22, 17.14, and 18.77 MeV for the total measured strength, then the ratio of experiment to theory is of the order of 0.7 for (p,p') and 0.5 for (e,e'). The (e,e') ratio will increase to 0.8 if the fragmented strength observed between 17.4 and 18 MeV is included in the total measured strength. The (p,p') ratio becomes larger than 1.0 if we include the strength observed at 14 MeV. If we limit the comparison only to the three well known 1^+ states, the (e,e') ratio of experiment to theory is smaller than the (p,p') ratio. This is a little surprising because in other light nuclei studied[30] the reverse situation is generally observed.

2. 2^- states

$M2$ transitions involve angular momentum transfers $\Delta L=1$ and 3. However, in intermediate energy (p,p') reactions at forward angles, the $\Delta L=1$ transfer dominates, giving a characteristic shape to the angular distribution (Fig. 3). The measured angular distributions for the known 2^-, $T=1$ and 2^-, $T=0$ states excited at 12.97 and 12.53 MeV are shown in Fig. 3 and compared with theoretical predictions. The calculated isoscalar 2^- angular distribution is flatter than the isovector one; this is due, in part, to the q dependence of the isoscalar spin part of the N-N interaction.

Except for the $E1$ structures observed at 22.3 and 24 MeV, all the states having an $L=1$ angular distribution are listed in Table VI and compared to the 2^- states measured in (e,e') (Refs. 6 and 28) and (^{3}He,t) (Ref. 32) reactions. By comparison with the (γ,n) spectrum [Fig. 2(b)], the broad structures at 20.4 and 20.9 MeV cannot be $E1$ transitions and must therefore correspond to 2^-, $T=1$ states. A 2^-, $T=1$ state is also observed in (e,e') (Ref. 28) at 20.3 MeV. The 20.4 MeV state (or the sum of the 20.4 and 20.9 MeV states) could be the analog of the broad 2^-, $T=1$ state observed in ^{16}F at 17.4 MeV in both the (^{3}He,t) (Ref. 32) and the (p,n) (Ref. 27) reactions. In the (e,e') experiment,[6] four additional 2^-, $T=1$ states have been observed at 16.82, 17.78, 18.50, and 19.00 MeV. In the charge exchange reaction only the analog of the 17.78 and 18.50 MeV states are excited. In the present experiment, we do not have any clear evidence for 2^-, $T=1$ states at these energies; only upper limits for the (p,p') cross section are given in Table VI. In the (e,e') experiment, the measured ratio $B(M2;\ 19.0\ \text{MeV})/B(M2;\ 12.97\ \text{MeV})$ is equal to 2.82 ± 0.10. The equivalent ratio for the measured (p,p') cross sections is smaller than 0.1. If the 19.0 MeV state observed in (e,e') is indeed a 2^- state, it would imply that this state is excited mainly by an orbital contribution; this has already been suggested in Ref. 6. The state at 12.53 MeV has been reported as a 2^-, $T=1$ state in the (e,e') experiment.[28] This state is listed as isoscalar in the table of levels of ^{16}O.[24] It has been shown[33] that there is at least 17% isospin mixing between the 2^- states at 12.53 and 12.97 MeV. This may explain why the shape of the measured (p,p') angular distribution for the 12.53 MeV state (shown in Fig. 3) lies between the calculated shape for isoscalar (solid line) and isovector (dashed line) 2^- angular distributions.

The 2^-, $T=1$ strength distributions measured in (p,p') and (e,e') experiments are compared to theoretical predic-

TABLE VI. 2^- states observed in ^{16}O and ^{18}O by different inelastic scattering experiments. † denotes the centroid of a broad structure.

	(p,p')[a]			(e,e')			(^{3}He,t)[d]		
	E_x (MeV)	$J^\pi;T$	$d\sigma/d\Omega(6°)$ (mb/sr)	E_x (MeV)	$J^\pi;T$	$B(M2)\uparrow$ (μ_N^2 fm^2)	E_x (in ^{16}F) (MeV)	$J^\pi;T$	S_{12} (fm^2)
^{16}O	8.87	$2^-;0$	0.032 ± 0.003						
	12.53	$2^-;0$	0.18 ± 0.01	12.53	$2^-;1$[b]	38 ± 9			
	12.97	$2^-;1$	0.74 ± 0.03	12.97	$2^-;1$[b]	121 ± 24	0.424	$2^-;1$	1.67
	16.82		≤0.065	16.82	$2^-;1$[c]	19 ± 2			
	17.78		≤0.050	17.78	$2^-;1$[c]	13 ± 3	5.274	$2^-;1$	0.13
	18.50		≤0.065	18.50	$2^-;1$[c]	59 ± 7	5.828	$2^-;1$	0.50
	19.00		≤0.065	19.00	$2^-;1$[c]	341 ± 51			
	$\langle20.40\rangle$†	$2^-;1$	1.25 ± 0.05	20.30	$2^-;1$[b]	461 ± 162	$\langle7.40\rangle$†	$2^-;1$	3.48
	$\langle20.90\rangle$†	$2^-;1$	0.33 ± 0.04						
^{18}O	16.39	$2^-;2$	0.345 ± 0.006	16.399 (±0.005)	$2^-;1$[c]	58 ± 7			

[a]This work.
[b]Reference 28.
[c]Reference 6 for ^{16}O and Ref. 7 for ^{18}O.
[d]Only on ^{16}O, Ref. 32.

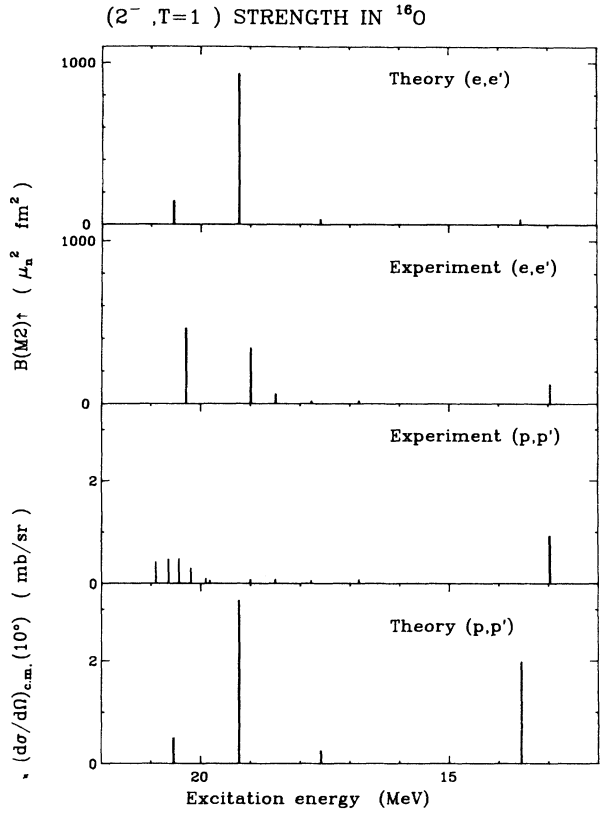

FIG. 5. Same as Fig. 4, but for 2^-, $T=1$ strength.

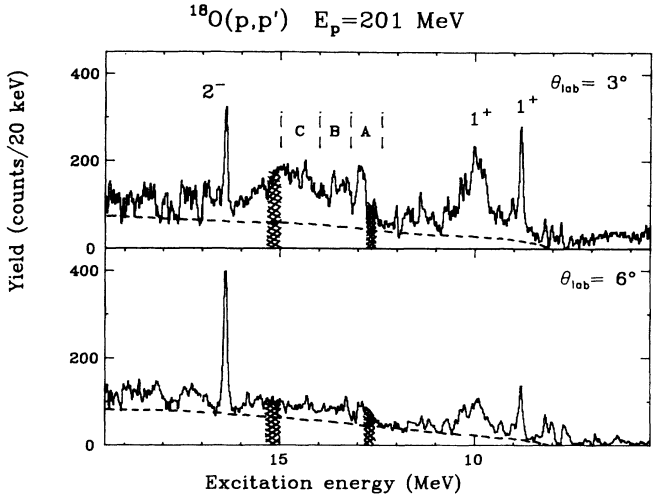

FIG. 6. $^{18}O(p,p')$ subtracted spectra at 3° and 6°. The excitation energy regions perturbed by the subtraction are cross hatched. The dashed curve corresponds to the empirically estimated continuum. See text for the definitions of *A*, *B*, and *C*.

tions in Fig. 5. The (p,p') strength at 20.4 MeV has been distributed over several single states to reproduce the shape of the resonance. The measured 2^-, $T=1$ strength distribution is reproduced quite well by the calculations. The ratio of the total observed strength to the total predicted strength up to 21 MeV of excitation energy is equal to 0.46 ± 0.04 for (p,p') and 0.79 ± 0.19 for (e,e'). If the 19.0 MeV state is assumed not to be a 2^- state, then the (e,e') ratio is reduced to 0.53 ± 0.16, which is in agreement with the (p,p') ratio.

The shell model calculations predict two strong 2^-, $T=0$ states at 14.9 and 17.6 MeV which are not observed experimentally. In the present experiment, a state at 14.9 MeV could have been missed because of the uncertainty associated with the subtraction of the strong 15.1 MeV carbon peak. The only experimentally known isoscalar 2^- states are that at 8.87 and possibly the state at 12.53 MeV. The ratio of the total observed 2^-, $T=0$ strength to the total predicted strength up to 21 MeV of excitation energy is equal to 0.10 ± 0.02 for (p,p').

3. 0^- states

A 0^-, $T=0$ state at 10.96 MeV and a 0^-, $T=1$ state at 12.79 MeV are reported in the table of levels of Ref. 24. These states have been studied recently in a 65 MeV $(\vec{p},p')$ experment.[34] In the present experiment, the cross section for the isovector state at 12.79 MeV could not be obtained because of its proximity to the 12.71 MeV state of ^{12}C. The angular distribution measured for the isoscalar 0^- state is given in Fig. 3. The shell model description of this state is almost a pure $(1p_{1/2}^{-1},2s_{1/2})$ configuration. The DWBA calculations were multiplied by 0.83 in order to reproduce the measured cross sections.

B. ^{18}O

Subtracted spectra obtained at 3° and 6° for the same integrated incident charge, and covering the excitation energy region from 5.5 to 19.5 MeV, are shown in Fig. 6. The 3° spectrum exhibits two well isolated sharp states at 8.82 and 16.40 MeV and many broad structures. Except for the 16.40 MeV state, which is a well known 2^-, $T=2$ state,[35] all the other structures seem to become smaller as the angle increases. Starting at the neutron threshold (8.04 MeV), an empirical continuum has been assumed, rising smoothly and joining the high energy region of the spectrum, as shown by the dashed lines in Fig. 6. The structure around 10 MeV can be analyzed as single levels for angles smaller than 6°; at larger angles the experimental energy resolution is not sufficient to resolve the structure into single states. Therefore, only the centroid energy and the total strength of the structure are given. The energies of the dominant single levels in the structure are 9.76, 9.89, 10.02, 10.27, 10.37, 10.67, and 10.80 MeV. The other broad structure, one that extends from 12.3 to 16 MeV, has large uncertainties near 12.7 and 15.1 MeV due to the subtraction of ^{12}C and ^{16}O peaks. The spectrum between 12 and 16 MeV has been analyzed in bins of 120 keV of excitation energy.

The (p,p') angular distributions measured for different transitions or regions of excitation energy are given in Figs. 7 and 8 and are compared in shape with theoretical predictions.

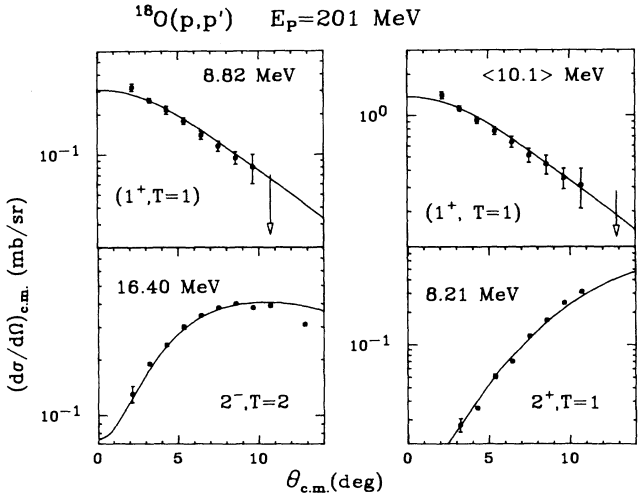

FIG. 7. Measured (p,p') angular distributions for some states in ^{18}O compared with microscopic DWBA calculations (see text for normalization factors).

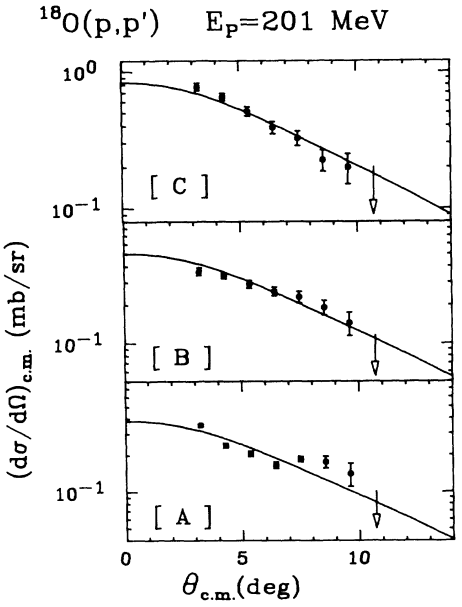

FIG. 8. Measured (p,p') differential cross sections for different excitation energy regions in ^{18}O (see Fig. 10) compared with microscopic DWBA calculations for the 1^+ state (see text for normalization factors).

1. 1^+ states

All the states, structures, and excitation energy regions having a forward peaked (p,p') angular distribution characteristic of an isovector 1^+ transition are listed in Table II and are compared to the results obtained in other reactions. In ^{18}O, isovector states can have either an isospin $T=1$ or 2. From the energy of the analog of the ground state of ^{18}N in ^{18}O, $T=2$ states are expected to occur at excitation energies greater than 16.2 MeV. Therefore, the state at 8.82 MeV and the broad structure having a centroid energy of 10.10 MeV are proposed to be 1^+, $T=1$ states. The excitation energy regions 12.4—13.2, 13.2—14, and 14—15 MeV, labeled [*A*], [*B*], and [*C*], respectively, contain significant amounts of possible 1^+, $T=1$ strength which is not observed in the other reactions. In fact, the only *M*1 transition reported in the detailed (e,e') analysis of ^{18}O between 11 and 27 MeV of excitation energy[7] corresponds to a 1^+, $T=2$ state at 18.87 MeV. No such 1^+ state is observed in the present experiment; only an upper limit for the (p,p') excitation of this state can be given.

As for ^{16}O, the (p,p') and (p,n) 1^+ cross sections measured, respectively, in ^{18}O and ^{18}F, are compared in Table III. In the charge exchange (p,n) reaction[36] on ^{18}O, $T=1$ Gamow-Teller transitions to states in ^{18}F are observed at 9.9, 10.9, and 11.9 MeV. The analog of these states in ^{18}O would be, respectively, the 8.82 MeV state and the structures around 9.8 and 10.8 MeV within the broad 10.1 MeV structure. For the 8.82 MeV state, the predicted and the observed (p,p') cross sections agree within the error bars. For the other structures the comparison is difficult because of the uncertainty in the state to state correspondence.

The 1^+, $T=1$ and 1^+, $T=2$ strength distributions measured in the present experiment and in the (e,e') experiment are compared with theoretical predictions in Fig. 9.

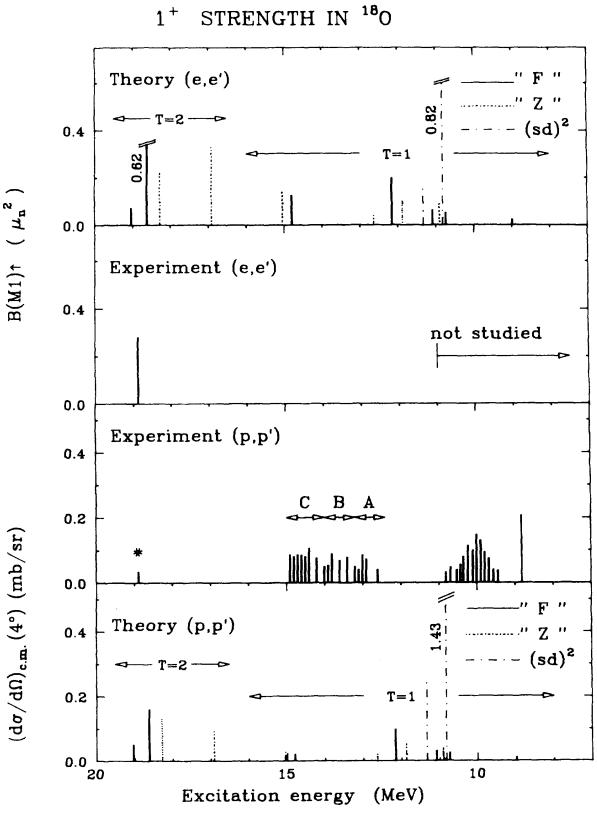

FIG. 9. (p,p') and (e,e') predicted strength distributions for 1^+, $T=1$ and 2 states in ^{18}O (see Sec. IV) compared with the measured ones [this work and Ref. 7 for (e,e')]. The asterisk indicates that the strength is an upper limit.

The calculations using the F and Z interactions predict the 1^+ strength due to the excitation of the ^{16}O core. The $T=1$ strength is fragmented between 10 and 15 MeV, and in both calculations the strongest predicted state is a $T=2$ state around 18.5 MeV. Significant orbital contributions are predicted for the $T=2$ states, interfering constructively with the spin contribution. The ratio of orbital to spin amplitudes can be as large as 0.8 (0.7) using the F (Z) interaction. The comparison between (e,e') and (p,p') results for the 18.87 MeV state indicates an important orbital contribution (see Table III) which is larger than the theoretical predictions.

The $(sd)^2$ calculations predict a large amount of 1^+, $T=1$ strength due to the two additional neutrons outside the ^{16}O core. This strength is concentrated in two states predicted at 10.82 and 11.34 MeV which can be related to the observed states at 8.82 and 10.10 MeV. The deduced spin transition probability $B(\sigma)$ for these states is given in Table IV. If these states are mainly neutron excitations, as predicted by the $(sd)^2$ calculations, they should be observed with the same transition probability in the (e,e') experiment. Unfortunately, the (e,e') experiment only studied the region above 16 MeV.

The measured 1^+, $T=1$ (p,p') strength and 1^+, $T=2$ (p,p') and (e,e') strengths for the individual structures are compared to the total predicted strength below 20 MeV in Table VII. If, in the total 1^+, $T=1$ measured strength, we include only the states at 8.82 and 10.10 MeV, then the ratio of experiment to theory is of the order of 0.7 for (p,p'). This ratio will double if we include the additional possible strength observed between 12 and 15 MeV. For the 1^+, $T=2$ strength, the (e,e') ratio is of the order of 0.4—0.5, depending on the interaction used in the predictions. Only an upper limit of 0.16 can be given for the (p,p') ratio.

2. 2^- states

The only 2^- transition observed in both the present experiment and the (e,e') experiment is the well known 2^-, $T=2$ state at 16.40 MeV. The measured (p,p') angular distribution is given in Fig. 7 and is very well reproduced in shape by the DWBA calculation. In good agreement with the experiment, the shell model calculations predict a strong 2^-, $T=2$ state at 17.04 MeV.

The ratio of experiment to theory for the 2^-, $T=2$ strength below 20 MeV of excitation energy is, respectively, 0.42 ± 0.04 for (p,p') and 0.28 ± 0.03 for (e,e').

VI. SUMMARY AND CONCLUSIONS

In the present (p,p') experiment, 1^+ and 2^- states are clearly excited in ^{16}O and ^{18}O. In ^{16}O, in addition to the well established 1^+ states at 16.22, 17.14, and 18.77 MeV, a broad structure centered at 14 MeV is observed with a (p,p') angular distribution characteristic of an isovector $M1$ transition. However, there is some doubt about the nature of this transition because of the disagreement with the (e,e'),[28] (p,n),[27] and (p,γ) (Ref. 8) results. In ^{18}O, a state at 8.82 MeV and a broad structure at 10.1 MeV are identified as $M1$ transitions. Additional possible $M1$ strength is found between 12 and 15 MeV.

The ratios of the orbital to spin amplitudes have been deduced for the 1^+ states by comparison with (e,e') results. In ^{16}O, only the 1^+ state at 16.22 MeV has an orbital contribution which is significant. In ^{18}O, the 1^+ state observed in (e,e') at 18.87 MeV is mainly due to orbital

TABLE VII. Ratio of the measured 1^+ strength to the total predicted strength (summed up to 20 MeV of excitation energy) for individual transitions and their sum, in ^{18}O. $[A]=12.4$—13.2 MeV, $[B]=13.2$—14.0 MeV, and $[C]=14.0$—15.0 MeV.

	Measured strength divided by total predicted strength for $M1$ states 1^+, $T=1$[a]		
E_x (MeV)	$(sd)^2$ (p,p')	$(sd)^2+F$ (p,p')	$(sd)^2+Z$ (p,p')
8.82	0.14	0.12	0.13
⟨10.10⟩	0.60	0.53	0.54
Total	0.74±0.04	0.65±0.03	0.67±0.03
$[A]$	0.17	0.15	0.15
$[B]$	0.22	0.19	0.20
$[C]$	0.37	0.33	0.33
Total including $[A]$, $[B]$, & $[C]$	1.50±0.12	1.32±0.10	1.35±0.10

	1^+, $T=2$[a,b]			
	F		Z	
E_x (MeV)	(p,p')	(e,e')	(p,p')	(e,e')
18.87	<0.15	0.41±0.06	<0.16	0.50±0.07

[a]This work.
[b](e,e'), Ref. 7.

excitation. For well separated 1^+ states with small uncertainty in the background subtraction, the measured (p,p') cross-sections are in excellent agreement with those predicted from the GT cross sections measured for the analog states in the (p,n) reaction.

The $M1$ and $M2$ strengths observed in the oxygen isotopes have been compared to shell model calculations. The agreement for the 1^+ strength in ^{16}O is good, given that the relatively simple model we have used leaves out one of the spin orbit partners. As shown in Ref. 8, previous 2p-2h calculations which include both spin-orbit partners give about the same total strength, but it is spread thinly over about a 25 MeV excitation energy range. The sensitivity to the interaction used in the complete 2p-2h space should be investigated, and it may be necessary to go up to 4p-4h or more in the basis to provide a consistent interpretation for the $M1$ strength. Given the simplicity of our F and Z calculations, we do not feel that too much significance should be attached to the details of the calculated strength distribution.

The $M1$ strength seen in ^{18}O in the $T=1$, 8.82 MeV and broad 10.1 MeV states in fairly well accounted for by just the $(sd)^2$ part of the calculation. The ratio of experimental cross sections to those predicted of 0.74 is somewhat larger than the ratio of 0.61 observed for the strong $A=18$ Gamow-Teller transitions.[37] The remaining $T=1$ strength in the A, B, and C regions is about twice as much as expected from the F and Z open-core calculations. However, we should keep in mind that the strength in the A, B, and C regions has only been observed in the (p,p') reaction. The $T=2$ strength at 18.87 MeV is very small in (p,p') compared to the calculations. This suggests that the strong (e,e') excitation observed at 18.87 MeV is mainly orbital in nature, in disagreement with the calculations.

The experimental strength distribution for the 2^-, $T=1$ states in ^{16}O is farily well reproduced by our calculation, with the strongest states being around 20 MeV. However, the large differences between the detailed strength distributions around 20 MeV in (p,p') and (e,e') are not reproduced by the calculation.

The overall quenching of about 0.5 (in both ^{16}O and ^{18}O) is probably due to higher-order configuration mixing ($\geq 3\hbar\omega$). The large difference between (p,p') and (e,e') for the lowest 2^-, $T=1$ state is reflected in the calculation. For the 2^-, $T=0$ strength the calculation indicates that there is considerable strength missing in the 15—18 MeV region. However, this strength may have been missed experimentally because these states are relatively weakly excited and may be broad.

ACKNOWLEDGMENT

This work was supported in part by the U.S. National Science Foundation under Grants PHY-80-17605 and INT-82-63242.

*On leave from Institut de Physique Nucléaire, Orsay, France.
†Present address: Donnelly Corporation, Holland, Michigan 49423.

[1] A. Richter, Nucl. Phys. **A374**, 177c (1983); Phys. Scr. **T5**, 63 (1983).
[2] U. E. P. Berg, in Proceedings of the International Symposium HESANS83 [J. Phys. (Paris) Colloq. **45**, C4-359 (1984)].
[3] C. Djalali, in Proceedings of the International Symposium HESANS83 [J. Phys. (Paris) Colloq. **45**, C4-375 (1984)].
[4] I. S. Towner and F. C. Khanna, Nucl. Phys. **A399**, 334 (1983); G. F. Bertsch and I. Hamamoto, Phys. Rev. C **26**, 1323 (1982).
[5] A. Bohr and B. Mottelson, Phys. Lett. **100B**, 10 (1981); A. Härting, W. Weise, H. Toki, and A. Richter, *ibid.* **104B**, 261 (1981).
[6] G. Küchler, A. Richter, E. Spamer, W. Steffen, and W. Knüpfer, Nucl. Phys. **A406**, 473 (1983).
[7] D. Bender, A. Richter, A. Spamer, E. J. Ansaldo, C. Rangacharyulu, and W. Knüpfer, Nucl. Phys. **A406**, 504 (1983).
[8] K. A. Snover, E. C. Adelberger, P. G. Ikossi, and B. A. Brown, Phys. Rev. C **27**, 1837 (1983).
[9] C. Djalali, thèse d'Etat, Université, Orsay, 1984 (unpublished).
[10] C. Djalali, N. Marty, M. Morlet, A. Willis, J. C. Jourdain, D. Böhle, U. Hartmann, G. Küchler, C. Caskey, G. M. Crawley, and A. Galonsky, Phys. Lett. **164B**, 269 (1985); C. Djalali and M. Morlet, in *Proceedings of the International Conference on Reaction Nuclear Mechanisms,* Varenna, 1985, edited by E. Gadioli (University of Milan, Milan, 1985), p. 401.
[11] C. Djajali, N. Marty, M. Morlet, and A. Willis, Nucl. Phys. **A280**, 42 (1982).
[12] D. J. Millener and D. Kurath, Nucl. Phys. **A255**, 315 (1975).
[13] B. S. Rehal and B. H. Wildenthal, Part. Nucl. **6**, 137 (1973); J. B. McGrory and B. H. Wildenthal, Phys. Rev. C **7**, 974 (1973).
[14] A. P. Zuker, Phys. Rev. Lett. **23**, 983 (1969).
[15] P. J. Ellis and L. Zamick, Ann. Phys. (N.Y.) **55**, 61 (1969).
[16] B. A. Brown, D. J. Horen, B. Castel, and H. Toki, Phys. Lett. **127B**, 151 (1983).
[17] B. H. Wildenthal, in *Progress in Particle and Nuclear Physics,* edited by D. H. Wilkinson (Pergamon, Oxford, 1984), Vol. 11, p. 5.
[18] R. Schaeffer and J. Raynal, program DWBA70 (unpublished).
[19] J. Comfort, program DW81 (unpublished).
[20] M. A. Franey and W. G. Love, Phys. Rev. C **31**, 488 (1985).
[21] V. Comparat, R. Frascaria, N. Marty, M. Morlet, and A. Willis, Nucl. Phys. **A221**, 403 (1974); V. Comparat, thèse d'Etat, Université Orsay, 1975 (unpublished).
[22] P. Schwandt, H. O. Meyer, W. W. Jacobs, A. D. Bacher, S. E. Vigdor, M. D. Kaitchuck, and T. R. Donoghue, Phys. Rev. C **31**, 55 (1982).
[23] C. D. Goodman, C. A. Goulding, M. B. Greenfield, J. Rapaport, D. E. Bainum, C. C. Foster, W. G. Love, and F. Petrovich, Phys. Rev. Lett. **26**, 1755 (1980).
[24] F. Ajzenberg-Selove, Nucl. Phys. **A375**, 1 (1982).
[25] R. L. Bramblett, J. T. Caldwell, R. R. Harvey, and S. C. Fultz, Phys. Rev. **133**, B869 (1964); R. A. Eramzhyan, B. S. Ishkanov, I. M. Kapitonov, and V. G. Neudatchin, Phys. Rep. **136**, 229 (1986).
[26] C. Djalali, N. Marty, M. Morlet, A. Willis, J. C. Jourdain, N. Anantaraman, G. M. Crawley, and A. Galonsky, Phys. Rev. C **31**, 758 (1985).
[27] A. Fazely, B. D. Anderson, M. Ahmad, A. R. Baldwin, A. M.

Kalenda, R. J. McCarthy, J. W. Watson, R. Madey, W. Bertozzi, T. N. Buti, J. M. Finn, M. A. Kovash, and B. Pugh, Phys. Rev. C **25**, 1760 (1982).

[28]M. Stroetzel and A. Goldman, Z. Phys. **233**, 245 (1970); A. Goldman and M. Stroetzel, *ibid.* **239**, 235 (1970).

[29]M. Buenerd, private communication.

[30]N. Anantaraman, B. A. Brown, G. M. Crawley, A. Galonsky, C. Djalali, N. Marty, M. Morlet, A. Willis, J. C. Jourdain, and B. H. Wildenthal, Phys. Rev. Lett. **31**, 1409 (1984); G. M. Crawley, private communication.

[31]B. D. Anderson, R. J. McCarthy, M. Ahmad, A. Fazely, A. M. Kalenda, J. N. Knudson, J. W. Watson, and C. C. Foster, Phys. Rev. C **26**, 8 (1982).

[32]S. Y. van der Werf, M. N. Harakeh, and W. A. Sterrenburg, contribution presented at the Fourth Amsterdam Miniconference, 1985 (unpublished).

[33]G. J. Wagner, K. T. Knöpfle, G. Mairle, P. Doll, H. Hafner, and J. L. C. Ford, Jr., Phys. Rev. C **16**, 1271 (1977).

[34]K. Hosono, M. Fujiwara, K. Hatanaka, K. Ikegami, M. Kondo, M. Matsuoka, T. Saito, S. Matsuki, K. Ogino, and S. Kato, Research Center for Nuclear Physics (Osaka) Annual Report 12, 1983.

[35]F. Ajzenberg-Selove, Nucl. Phys. **A300**, 1 (1978).

[36]B. D. Anderson, A. Fazely, R. J. McCarthy, P. C. Tandy, J. W. Watson, R. Madey, W. Bertozzi, T. N. Buti, J. M. Finn, J. Kelly, M. A. Kovash, B. Pugh, B. H. Wildenthal, and C. C. Foster, Phys. Rev. C **27**, 1387 (1983).

[37]B. A. Brown and B. H. Wildenthal, At. Data Nucl. Data Tables **33**, 347 (1985).

[38]J. W. Watson, W. Pairsuwan, B. D. Anderson, A. R. Baldwin, B. S. Flanders, R. Madey, R. J. McCarthy, B. A. Brown, B. H. Wildenthal, and C. C. Foster, Phys. Rev. Lett. **55**, 1369 (1985).